satellites can be useful for probing dynamic processes involving the metal–selenium bonds.[8] Only satellites arising from trans $^{31}P-^{77}Se$ coupling are clearly observed in the Pd and Pt complexes. The cis coupling is too small (<10 Hz), and the satellite arising from these are in the base of the main peak.

Acknowledgment. We wish to thank the Department of Pharmacology and Dr. Thomas Gerken for running a number of samples on the Bruker WP 180. The National Institutes of Health, Grant GM-19050, and the National Science Foundation, Grant CHE 76-18709, have supported these studies.

Registry No. $K(Se_2CN(i\text{-}Bu)_2)$, 67994-90-5; $CH_2(Se_2CN(i\text{-}Bu)_2)_2$, 76137-25-2; $Zn(Se_2CNEt_2)_2$, 19400-58-9; $Zn(Se_2CN(i\text{-}Bu)_2)_2$, 68011-63-2; $(NH_2Et_2)Se_2CNEt_2$, 30634-02-7; $Ni(Se_2CNEt_2)_2$, 19400-59-0; $Ni(Se_2CN(i\text{-}Bu)_2)$, 68025-77-4; $Ni(Se_2CNEt_2)PEt_3Cl$, 67994-91-6; $Ni(Se_2CNEt_2)PMePh_2Cl$, 76136-18-0; $Pd(Se_2CN(i\text{-}Bu)_2)_2$, 68011-58-5; $Pd(Se_2CNEt_2)PEt_3Cl$, 76136-19-1; $Pd(Se_2CNEt_2)PPh_3Cl$, 76136-20-4; $Pd(Se_2CN(i\text{-}Bu)_2)PPh_3Cl$, 68025-79-6; $Pt(Se_2CNEt_2)_2$, 19400-65-8; $Pt(Se_2CN(i\text{-}Bu)_2)_2$, 68025-75-2; $Pt(Se_2CNEt_2)PPh_3Cl$, 68011-59-6; $Pt(Se_2CN(i\text{-}Bu)_2)PPh_3Cl$, 68252-96-0; $Pt(Se_2CNEt_2)PPh_3CH_3$, 76136-21-5; $Pt(Se_2CNEt_2)PPh_3I$, 76136-22-6; $[Pt(Se_2CN(i\text{-}Bu)_2)(PPh_3)_2]Cl$, 68025-78-5; $[Pt(Se_2CN(i\text{-}Bu)_2)_3]Cl$, 76136-23-7; *cis*-$Pt(Se_2CN(i\text{-}Bu)_2)_2I_2$, 68011-50-7; *cis*-$Pt(Se_2CN(i\text{-}Bu)_2)_2Br_2$, 68011-61-0; $Co(Se_2CNEt_2)_3$, 76136-24-8; $Pd(Se_2CNEt_2)_2$, 19400-60-3; $Ni(PEt_3)_2Cl_2$, 17523-24-9; $Pd(PPh_3)_2Cl_2$, 13965-03-2; $Pt(PPh_3)_2Cl_2$, 10199-34-5; $Pt(PPh_3)_2(CH_3)_2$, 17567-35-0; K_2PtCl_4, 10025-99-7; $(N(i\text{-}Bu)_2H_2)Se_2CN(i\text{-}Bu)_2$, 76137-27-4.

Supplementary Material Available: A listing of observed and calculated structure factor amplitudes (4 pages). Ordering information is given on any current masthead page.

Contribution from the Department of Chemistry, University of Virginia, Charlottesville, Virginia 22901

Mercury-Bridged Cobaltacarborane Complexes Containing B–Hg–B Three-Center Bonds. Synthesis and Structure of μ,μ'-$[(\eta^5\text{-}C_5R_5)Co(CH_3)_2C_2B_3H_4]_2Hg$ and μ-$[(\eta^5\text{-}C_5R_5)Co(CH_3)_2C_2B_3H_4]HgCl$ (R = H, CH_3) and Related Compounds[1]

DAVID C. FINSTER and RUSSELL N. GRIMES*

Received September 9, 1980

Reactions of the *nido*-cobaltacarborane anions $(\eta^5\text{-}C_5H_5)Co(CH_3)_2C_2B_3H_4^-$ and $[\eta^5\text{-}C_5(CH_3)_5]Co(CH_3)_2C_2B_3H_4^-$ with $HgCl_2$ in tetrahydrofuran give initially the unstable adducts $[(\eta^5\text{-}C_5R_5)Co(CH_3)_2C_2B_3H_4\cdot HgCl_2]^-$ (R = H, CH_3), which lose Cl^- to form the isolable HgCl-bridged complexes μ-$[(\eta^5\text{-}C_5R_5)Co(CH_3)_2C_2B_3H_4]HgCl$; the latter species undergo symmetrization to generate the bis(cobaltacarboranyl)mercury complexes μ,μ'-$[(\eta^5\text{-}C_5R_5)Co(CH_3)_2C_2B_3H_4]_2Hg$. In the cyclopentadienyl system (R = H), the formation of the μ,μ' complex is rapid, giving high yields within minutes; in contrast, the pentamethylcyclopentadienyl species reacts much more slowly, requiring days to form the μ,μ' complex in isolable quantity. Thus, the characterization of the mono(cobaltacarboranyl)mercury complex is readily achieved with the $C_5(CH_3)_5$-substituted cobaltacarborane. The structural characterization of the Hg-bridged complexes is based on pulse Fourier transform ^1H and ^{11}B NMR, IR, and mass spectra, and single-crystal X-ray diffraction studies of μ-$[[\eta^5\text{-}C_5(CH_3)_5]Co(CH_3)_2C_2B_3H_4]HgCl$ and μ,μ'-$[(\eta^5\text{-}C_5H_5)Co(CH_3)_2C_2B_3H_4]_2Hg$. The mono(cobaltacarboranyl) complex crystallizes as a dimer with weak intermolecular Hg···Cl interactions. Crystal data for $HgCoClC_{14}B_3H_{25}$: mol wt 520.76, space group $P2_1/n$, $Z = 2$, $a = 9.634$ (2) Å, $b = 14.05$ (1) Å, $c = 13.862$ (7) Å, $\beta = 96.71$ (3)°, $V = 1863$ Å^3, $R = 0.044$ for 1607 reflections having $F_o^2 > 3\sigma(F_o^2)$. Crystal data for $HgCo_2C_{18}B_6H_{30}$: mol wt 629.75, space group $P2_1/n$, $Z = 2$, $a = 8.456$ (8) Å, $b = 11.334$ (7) Å, $c = 11.77$ (1) Å, $\beta = 100.12$ (9)°, $V = 1110$ Å^3, $R = 0.081$ for 1441 reflections having $F_o^2 > 3\sigma(F_o^2)$.

Introduction

A recent report[2] from these laboratories described the preparation of the mercury-bridged complexes μ,μ'-$[(CH_3)_2C_2B_4H_5]_2Hg$ (I), μ,μ'-$(B_5H_8)_2Hg$ (II), and some chemistry based on these species. In the proposed structures[2] of I and II, a mercury atom interacts with a B–B edge on the open face of the *nido*-carborane or -borane ligand, forming a two-electron, three-center B–Hg–B bond. The general principle of boron–metal–boron bridging in nido-boranes and -carboranes is well established;[3] in addition to I and II, there are several known complexes in which a metal (or nonmetal) atom participates in B–M–B bridge-bonding on *two* separate ligands.[4] However, previous examples of well-characterized B–Hg–B bridging are virtually nonexistent.[5]

(1) Based in part on a Ph.D. dissertation, University of Virginia, 1980, by D.C.F.
(2) Hosmane, N. S.; Grimes, R. N. *Inorg. Chem.* **1979**, *18*, 2886.
(3) (a) Greenwood, N. N.; Ward, I. M. *Chem. Soc. Rev.* **1974**, *3*, 231. (b) Wegner, P. A. In "Boron Hydride Chemistry"; Muetterties, E. L., Ed.; Academic Press: New York, 1975; Chapter 12.
(4) (a) Tabereaux, A.; Grimes, R. N. *Inorg. Chem.* **1973**, *12*, 792. (b) Davison, A.; Traficante, D. D.; Wreford, S. S. *J. Am. Chem. Soc.* **1974**, *96*, 2802. (c) Denton, D. L.; Clayton, W. R.; Mangion, M.; Shore, S. G.; Meyers, E. A. *Inorg. Chem.* **1976**, *15*, 541. (d) Brennan, J. P.; Schaeffer, R.; Davison, A.; Wreford, S. S. *J. Chem. Soc., Chem. Commun.* **1973**, 354. (e) Shore, S. G. "Abstracts of Papers", 19th International Conference on Coordination Chemistry, Prague, Czechoslovakia, Sept 1978. (f) Greenwood, N. N.; Hails, M. J.; Kennedy, J. D.; McDonald, W. S. *J. Chem. Soc., Chem. Commun.* **1980**, 37. (g) Greenwood, N. N.; McGinnety, J. A.; Owen, J. D. *J. Chem. Soc., Dalton Trans.* **1972**, 989. (h) Guggenberger, L. J. *J. Am. Chem. Soc.* **1972**, *94*, 114.
(5) In the known mercury complexes of the *nido*-$B_{10}H_{12}^{2-}$ ligand,[6] Hg is evidently η^4-coordinated to the cage, and in the complexes of *nido*-$C_2B_9H_{11}^{2-}$ and *closo*-$C_2B_{10}H_{11}^-$ it is η^1-coordinate (σ bonded).[7,8] A partially characterized complex formulated as μ-(C_6H_5Hg)-2,3-$C_2B_4H_7$ was reported several years ago.[9]
(6) (a) Greenwood, N. N.; Thomas, B. S.; Waite, D. W. *J. Chem. Soc., Dalton Trans.* **1975**, 299. (b) Greenwood, N. N.; Sharrocks, D. N. *J. Chem. Soc. A* **1969**, 2334. (c) Greenwood, N. N. *Pure Appl. Chem.* **1977**, *49*, 791.

0020-1669/81/1320-0863$01.00/0

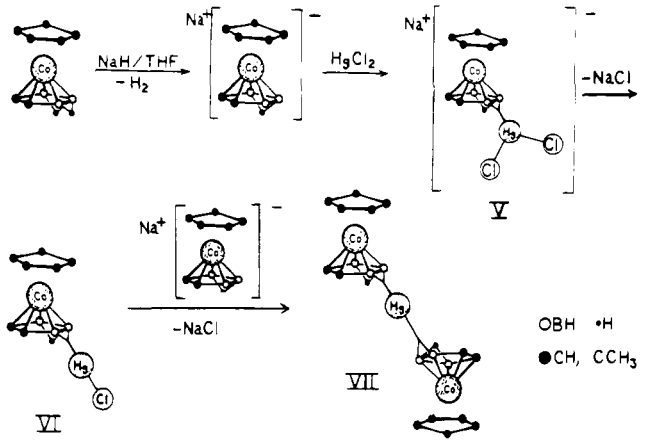

Figure 1. Reaction sequence for complexation of cobaltacarborane anions with $HgCl_2$. Product yields are given in Table I.

Table I. Yields of Mercury-Bridged Cobaltacarboranes[a,b]

R	reacn time	V	VI	VII
H	10 min	t	t	66
H	4 days	t	t	t
CH_3	10 min	19	4	t
CH_3	2 days	t	31	27

[a] Yields given as percent of theoretical on the basis of amount of starting cobaltacarborane consumed; t = trace. [b] Key: V, $Na^+[\mu\text{-}(\eta^5\text{-}C_5R_5)Co(CH_3)_2C_2B_3H_4\cdot HgCl_2]^-$ (VA, R = H; VB, R = CH_3); VI, $\mu\text{-}[(\eta^5\text{-}C_5R_5)Co(CH_3)_2C_2B_3H_4]HgCl$ (VIA, R = H; VIB, R = CH_3); VII, $\mu,\mu'\text{-}[(\eta^5\text{-}C_5R_5)Co(CH_3)_2C_2B_3H_4]_2Hg$ (VIIA, R = H; VIIB, R = CH_3).

The cobaltacarboranes 1,2,3-$(\eta^5\text{-}C_5R_5)Co(CH_3)_2C_2B_3H_5$ (III, R = H;[10] IV, R = CH_3[11]) are direct analogues of the nido-carborane $(CH_3)_2C_2B_4H_6$ in which a $Co(C_5R_5)$ unit replaces the apex BH, and are readily available to us. Hence it appeared worthwhile to explore the synthesis of mercury-bridged derivatives of III and IV (which would be analogues of complex I, mentioned above) in order to assess the influence of the apical $Co(C_5R_5)$ unit on complexation. An additional motivation was the hope of producing crystals of mercury-bridged complexes suitable for X-ray diffraction studies, inasmuch as no definitive structural characterization of a complex containing discrete B–Hg–B three-center bridges had been reported.

Results and Discussion

Synthesis of Mercury-Bridged Cobaltacarboranes. As has been described previously,[10] the *nido*-cobaltacarborane 1,2,3-$(\eta^5\text{-}C_5H_5)Co(CH_3)_2C_2B_3H_5$ (III) reacts easily with sodium hydride in tetrahydrofuran (THF) at room temperature, eliminating one of its two bridging protons to form the $(C_5H_5)Co(CH_3)_2C_2B_3H_4^-$ anion (Figure 1); the reaction is analogous to the bridge-deprotonation[12] of 2,3-$C_2B_4H_8$ to give $C_2B_4H_7^-$. The pentamethylcyclopentadienyl counterpart, IV, also undergoes bridge deprotonation but much more slowly (i.e., a matter of hours for IV vs. min in the case of III). Treatment of the $(\eta^5\text{-}C_5R_5)Co(CH_3)_2C_2B_3H_4^-$ anions (R = H or CH_3) with $HgCl_2$ in THF proceeds as shown in Figure 1, generating initially an $HgCl_2$-bridged unstable intermediate VA (R = H) or VB (R = CH_3); these species in turn lose Cl^- to give the corresponding yellow-orange HgCl-bridged complexes VIA and VIB.

Further reaction of VIA and VIB with a second molar equivalent of the cobaltacarborane anion produces the respective yellow-orange μ,μ'-bis(cobaltacarboranyl) complexes VIIA and VIIB; again, there is a notable difference in the reactivity of the $C_5H_5^-$ vs. the $C_5(CH_3)_5^-$-containing species, with the former (VIA) adding a second cobaltacarborane

Table II. 32.1-MHz ^{11}B NMR Data

compd	solvent	chem shifts (rel area)[a]
VIIA	$CDCl_3$	8.8 (2)
		2.8 (1)
VIB	$CDCl_3$	12.2 (1)
		7.5 (2)
VIB	C_6D_6	10.2 (2)
		5.0 (1)
VIIB	$CDCl_3$	13.6 (2)
		8.5 (1)

[a] In ppm and vs. $BF_3\cdot O(C_2H_5)_2$; positive shifts downfield. J_{BH} coupling constants not readily determined due to peak overlap.

Table III. 100-MHz ^1H NMR Data

compd (solvent)	chem shift[a] (rel area)	assignt[b]
VIIA ($CDCl_3$)	4.68 (5)	C_5H_5
	3.60 (1)	BH
	3.44 (1)	BH
	3.03 (1)	BH
	1.89 (3)	CH_3
	1.75 (3)	CH_3
	−6.37 (1)[b]	BHB
VIB (C_6D_6)	3.21 (2)	BH
	2.65 (1)	BH
	1.38[c]	CH_3 (cage and ring)
	−5.58 (1)[d]	BHB
VIIB (C_6D_6)	3.68 (1)	BH
	3.26 (1)	BH
	2.94 (1)	BH
	1.60 (6)	CH_3 (cage)
	1.56 (15)	CH_3 (ring)
	−5.51 (1)	BHB
VB (C_6D_6)	3.5 (2)	BH
	3.3 (1)	BH
	1.93 (3)	CH_3 (cage)
	1.62 (15)	CH_3 (ring)
	1.59 (3)	CH_3 (cage)
	−5.1 (1)	BHB

[a] In ppm vs. Me_4Si. [b] ^{199}Hg satellites at $^2J_{HgH}$ = 113 Hz. [c] Integration not clear due to impurities. [d] ^{199}Hg satellites at $^2J_{HgH}$ = 67 Hz.

Table IV. IR Absorptions (cm^{-1}; KBr pellets)[a]

$\mu\text{-}(\eta^5\text{-}C_5(CH_3)_5)Co(CH_3)_2C_2B_3H_4HgCl$ (VIB)
2950 sh, 2910 s, 2860 s, 2540 sh, 2515 s, 1850 m, 1730 m, 1585 m, 1560 s, br, 1380 s, 1265 w, 1075 m, 1025 s, 1015 s, 1000 s, 990 w, 950 w, 910 s, 785 s, 735 s, 650 m

$\mu\text{-}[(\eta^5\text{-}C_5H_5)Co(CH_3)_2C_2B_3H_4]_2Hg$ (VIIA)
2930 m, 2900 m, 2850 m, 2510 s, 2435 s, 1830 sh, 1815 m, 1580 s, 1415 m, 1360 m, 1350 m, 1110 m, 1000 s, 950 s, 890 w, 840 m, 820 s, 780 w, 760 w, 695 s

$\mu\text{-}[\eta^5\text{-}(C_5(CH_3)_5)Co(CH_3)_2C_2B_3H_4]_2Hg$ (VIIB)
2950 sh, 2900 s, 2860 sh, 2485 s, 2415 s, 1815 m, 1555 m, 1460 s, br, 1375 s, 1360 sh, 1260 w, 1070 m, 1025 s, 1000 s, 945 s, 885 w, 840 s, 800 m, 755 m, 695 s

[a] Key: s = strong, m = medium, w = weak, br = broad, sh = shoulder.

(7) (a) Colquhoun, H. M.; Greenhough, T. J.; Wallbridge, M. G. H. *J. Chem. Soc., Chem. Commun.* **1977**, 737. (b) Colquhoun, H. M.; Greenhough, T. J.; Wallbridge, M. G. H. *J. Chem. Soc., Dalton Trans.* **1979**, 619.
(8) See ref 2, footnote 8.
(9) Magee, C. P.; Sneddon, L. G.; Beer, D. C.; Grimes, R. N. *J. Organomet. Chem.* **1975**, *86*, 159.
(10) Grimes, R. N.; Beer, D. C.; Sneddon, L. G.; Miller, V. R.; Weiss, R. *Inorg. Chem.* **1974**, *13*, 1138.
(11) Finster, D. C.; Sinn, E.; Grimes, R. N. *J. Am. Chem. Soc.*, in press.
(12) Onak, T.; Dunks, G. B. *Inorg. Chem.* **1966**, *5*, 439.

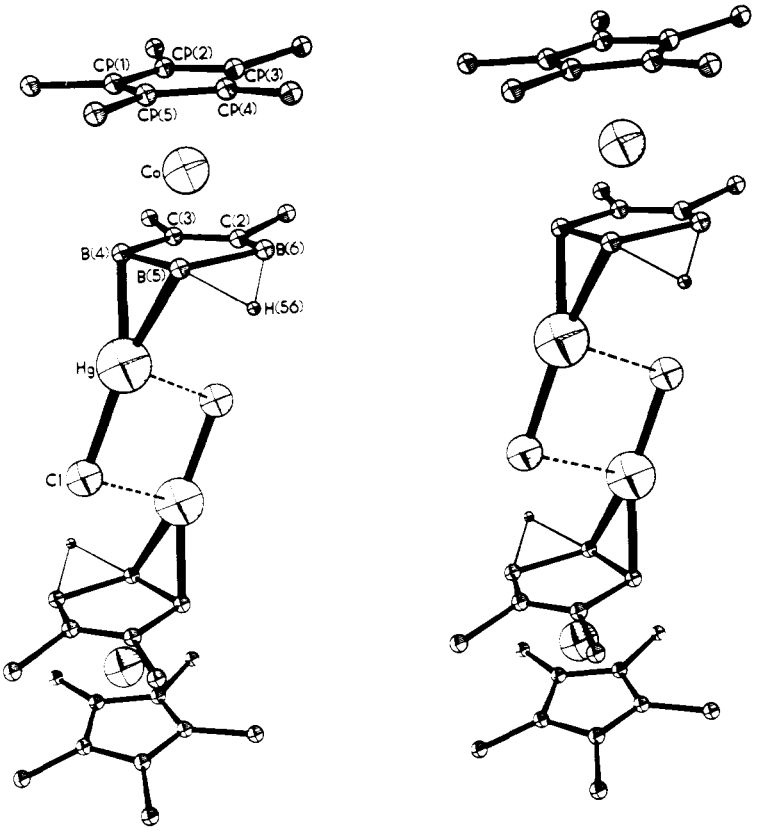

Figure 2. Stereoview of the molecular structure of VIB, with atoms shown as spheres of arbitrary radius. The weak intermolecular Hg···Cl interactions are represented by dashed lines.

ligand much more rapidly (Table I). As a consequence, the HgCl-bridged $C_5(CH_3)_5$ derivative (VIB) was isolated and fully characterized, whereas its cyclopentadienyl counterpart (VIA) was detected only in trace amounts. Similarly, the C_5H_5 complex VIIA was generated rapidly in high yield while the $C_5(CH_3)_5^-$-containing species VIIB required days to form in isolable quantity (Table I). The unstable $HgCl_2$-bridged intermediates (VA and VB) were only partially characterized from mass spectral and (in the case of VB) proton NMR data as described below.

Spectroscopic Characterization. The ^{11}B and ^1H FT NMR data (Tables II and III) and IR spectra (Table IV) of the three isolable species VIB, VIIA, and VIIB are consistent with, but do not in themselves confirm, the structures shown in Figure 1. The ambiguity arises, in part, from the fact that the bridging mercury atom does not cause major perturbations in chemical shifts relative to those of the parent (unbridged) cobaltaborane;[10,11] thus, the ^{11}B NMR spectra exhibit only two resonances in a 2:1 area ratio instead of the expected three equal-area signals. However, the inequivalence of the cage C–CH_3 units is evident in the proton spectra of VB and VIIA, and the split B–H absorption near 2500 cm^{-1} in the IR spectra of the compounds is characteristic of heteroatom-bridged derivatives of *nido*-carboranes.[2,13] The structures of these compounds were unequivocally established from X-ray crystal structure analyses of VIB and VIIA, as described in the following section.

The geometries of the proposed $HgCl_2$-bridged anionic intermediates VA and VB, shown in Figure 1, are not certain but are suggested by the conditions of synthesis and the known structures of subsequent products. These species are evidently salts in view of their low TLC R_f values (0.05–0.2 in 1:1 CH_2Cl_2/hexane) and the absence of mass spectral peaks at probe temperatures less than ~290 °C (neutral metallacarboranes typically have sufficient volatility to exhibit mass spectra below 200 °C). The mass spectra obtained for VA and VB at 290 °C exhibit high-mass cutoffs at *m/e* 700 and 840, respectively, corresponding to $(C_5R_5)_2Co_2(CH_3)_4C_4B_6H_4Cl_2Hg^+$ ions (R = H, CH_3), which are assumed to form by pyrolysis of the ionic samples; the presence of $(C_5R_5)Co(CH_3)_2C_2B_3H_3^+$ and Hg^+ fragments is clearly evident. The 100-MHz ^1H FT NMR spectrum of VB is consistent with an Hg-bridged CoC_2B_4 complex and is very similar to that of the structurally established species VIB which forms from VB on standing. Thus, complexes VA and VB are formulated as Na^+ salts of $HgCl_2$-bridged adducts[14] of the respective $[(C_5R_5)Co(CH_3)_2C_2B_3H_4{\cdot}HgCl_2]^-$ anions with the proposed structures depicted in Figure 1.

Molecular Structures of μ-[[η^5-$C_5(CH_3)_5$]Co-$(CH_3)_2C_2B_3H_4$]HgCl (VIB) and μ,μ'-[(η^5-C_5H_5)Co-$(CH_3)_2C_2B_3H_4]_2$Hg (VIIA). The geometries and unit cell packing of VIB and VIIA are shown in Figures 2–5, and the relevant crystallographic data are given in Tables V–IX. The molecular structures of both compounds conform to those proposed from spectroscopic data and contain a mercury atom bridging a B–B edge on the open face of a pyramidal CoC_2B_3 unit. In the HgCl-bridged species VIB, the two enantiomeric forms of the molecule crystallize in centrosymmetric pairs (Figure 2) with the HgCl moieties parallel to each other and within weakly bonding distance [3.155 (3) Å]; this intermolecular Hg–Cl separation can be compared with the *intra*molecular Hg–Cl distance of 2.349 (3) Å, which reflects strong covalent bonding. The dimerization of VIB in the solid state is not unusual, since many organomercury compounds adopt crystal structures in which there are weak intermolecular

(13) See papers cited in ref 2, footnote 2.

(14) Adducts of $HgCl_2$ with organic sulfides and with organometallics such as (η^5-C_5H_5)$(CO)_2Co$ are known: Cotton, F. A.; Wilkinson, G. "Advanced Inorganic Chemistry", 4th ed.; Wiley: New York, 1980; pp 607–608 and references cited therein.

Table V. Positional and Thermal Parameters and Their Estimated Standard Deviations for μ-[(η^5-$C_5(CH_3)_5$)Co(CH_3)$_2C_2B_3H_4$]HgCl[a]

atom	x	y	z	U_{11}	U_{22}	U_{33}	U_{12}	U_{13}	U_{23}
Hg	0.14758 (7)	0.10274 (5)	−0.01295 (5)	0.0744 (3)	0.0859 (4)	0.0944 (4)	−0.0181 (4)	−0.0163 (3)	0.0462 (3)
Co	0.1475 (2)	0.3113 (1)	−0.1975 (1)	0.060 (1)	0.056 (1)	0.053 (1)	−0.006 (1)	0.0011 (9)	0.0115 (9)
Cl	0.1442 (5)	−0.0201 (3)	0.1018 (3)	0.115 (3)	0.113 (3)	0.127 (3)	−0.046 (3)	−0.045 (3)	0.078 (2)
C(P1)	0.225 (2)	0.443 (1)	−0.155 (1)	0.082 (10)	0.07 (1)	0.104 (13)	−0.017 (9)	0.023 (9)	0.005 (10)
C(P2)	0.120 (2)	0.456 (1)	−0.225 (1)	0.077 (10)	0.06 (1)	0.140 (14)	0.001 (9)	0.025 (10)	0.041 (10)
C(P3)	0.149 (2)	0.407 (1)	−0.310 (1)	0.096 (11)	0.11 (1)	0.080 (10)	−0.028 (10)	−0.023 (9)	0.057 (9)
C(P4)	0.284 (2)	0.362 (1)	−0.285 (1)	0.124 (11)	0.09 (1)	0.079 (10)	−0.007 (10)	0.061 (8)	0.009 (9)
C(P5)	0.326 (1)	0.391 (1)	−0.189 (1)	0.051 (8)	0.08 (1)	0.099 (10)	−0.010 (8)	0.007 (7)	0.042 (9)
C(M1)	0.234 (3)	0.489 (1)	−0.051 (2)	0.260 (22)	0.11 (1)	0.137 (16)	−0.092 (15)	0.077 (15)	−0.050 (13)
C(M2)	−0.011 (2)	0.516 (2)	−0.224 (2)	0.097 (12)	0.11 (2)	0.325 (29)	0.044 (11)	0.078 (14)	0.070 (18)
C(M3)	0.063 (3)	0.410 (2)	−0.408 (2)	0.219 (24)	0.25 (3)	0.104 (15)	−0.063 (22)	−0.067 (15)	0.055 (19)
C(M4)	0.365 (2)	0.307 (2)	−0.351 (2)	0.229 (18)	0.18 (2)	0.152 (15)	0.010 (18)	0.126 (12)	−0.043 (16)
C(M5)	0.471 (2)	0.366 (2)	−0.125 (2)	0.077 (12)	0.19 (2)	0.264 (26)	−0.039 (13)	−0.055 (14)	0.104 (19)
C(2)	−0.013 (2)	0.217 (1)	−0.228 (1)	0.183 (15)	0.10 (1)	0.042 (9)	−0.079 (10)	−0.020 (10)	0.015 (8)
C(3)	−0.025 (1)	0.260 (1)	−0.142 (1)	0.071 (9)	0.10 (1)	0.105 (11)	0.005 (9)	0.034 (8)	0.046 (10)
C(B2)	−0.150 (2)	0.236 (2)	−0.309 (2)	0.191 (15)	0.20 (2)	0.189 (18)	−0.107 (14)	−0.131 (12)	0.054 (18)
C(B3)	−0.146 (2)	0.316 (2)	−0.116 (2)	0.126 (13)	0.12 (2)	0.228 (21)	0.040 (13)	0.094 (12)	0.050 (17)
B(4)	0.120 (2)	0.249 (1)	−0.069 (1)	0.09 (1)	0.07 (1)	0.08 (1)	−0.01 (1)	0.02 (1)	0.01 (1)
B(5)	0.222 (2)	0.186 (1)	−0.139 (2)	0.12 (1)	0.06 (1)	0.12 (2)	0.03 (1)	0.03 (1)	0.05 (1)
B(6)	0.116 (3)	0.174 (2)	−0.254 (3)	0.24 (3)	0.10 (2)	0.33 (3)	0.03 (2)	0.15 (2)	0.09 (2)
H(56)	0.19 (2)	0.10 (1)	−0.21 (1)						

[a] The form of the anisotropic thermal parameter is $\exp[-2\pi^2(U_{11}h^2a^{*2} + U_{22}k^2b^{*2} + U_{33}l^2c^{*2} + 2U_{12}hka^*b^* + 2U_{13}hla^*c^* + 2U_{23}klb^*c^*)]$. For hydrogen atom, standard isotropic B value is 9 (5) Å^2. Atoms C(B2) and C(B3) are the methyl carbons attached to C(2) and C(3), respectively; atoms C(M1)–C(M5) are the methyl carbons attached to C(P1)–C(P5), respectively.

Table VI. Positional and Thermal Parameters and Their Estimated Standard Deviations for μ,μ'-[(η^5-C_5H_5)Co(CH_3)$_2C_2B_3H_4$]$_2$Hg[a]

atom	x	y	z	U_{11}	U_{22}	U_{33}	U_{12}	U_{13}	U_{23}
Hg	0.0000	0.0000	0.0000	0.0546 (5)	0.0464 (4)	0.0415 (4)	0.0078 (5)	−0.0095 (4)	−0.0081 (5)
Co	0.0110 (2)	0.1926 (2)	0.2838 (2)	0.040 (1)	0.035 (1)	0.046 (1)	0.002 (1)	0.0001 (8)	−0.006 (1)
C(2)	0.175 (2)	0.058 (1)	0.315 (1)	0.038 (8)	0.038 (8)	0.050 (8)	0.007 (7)	0.003 (7)	−0.001 (8)
C(3)	0.212 (2)	0.133 (1)	0.226 (1)	0.036 (8)	0.041 (9)	0.064 (9)	0.002 (7)	0.007 (7)	−0.008 (8)
C(M2)	0.294 (2)	0.045 (2)	0.429 (2)	0.048 (10)	0.096 (13)	0.060 (10)	0.013 (10)	−0.020 (9)	0.022 (10)
C(M3)	0.371 (2)	0.194 (2)	0.237 (2)	0.050 (9)	0.072 (12)	0.082 (11)	−0.023 (10)	0.017 (8)	−0.019 (10)
C(P1)	0.060 (2)	0.361 (2)	0.341 (2)	0.063 (12)	0.053 (11)	0.134 (17)	−0.012 (10)	0.015 (11)	−0.035 (11)
C(P2)	−0.077 (2)	0.361 (2)	0.263 (2)	0.091 (13)	0.047 (10)	0.080 (12)	0.028 (10)	0.012 (10)	−0.012 (9)
C(P3)	−0.185 (2)	0.288 (2)	0.303 (2)	0.054 (11)	0.073 (14)	0.150 (19)	0.002 (11)	0.019 (12)	−0.027 (14)
C(P4)	−0.122 (3)	0.246 (2)	0.403 (2)	0.163 (14)	0.066 (13)	0.123 (11)	−0.007 (12)	0.113 (9)	−0.006 (11)
C(P5)	0.035 (3)	0.288 (2)	0.434 (2)	0.166 (22)	0.082 (15)	0.043 (10)	0.039 (15)	−0.001 (12)	−0.008 (11)
B(4)	0.063 (2)	0.153 (2)	0.126 (1)	0.070 (12)	0.04 (1)	0.030 (8)	−0.005 (9)	0.001 (8)	−0.003 (7)
B(5)	−0.094 (2)	0.073 (2)	0.163 (2)	0.054 (11)	0.04 (1)	0.053 (10)	−0.004 (10)	−0.007 (9)	−0.009 (9)
B(6)	0.005 (2)	0.011 (2)	0.303 (2)	0.046 (9)	0.05 (1)	0.048 (9)	0.000 (10)	0.003 (8)	−0.010 (9)

atom	x	y	z	B, Å^2	atom	x	y	z	B, Å^2
H(56)	−0.06 (2)	−0.06 (2)	0.18 (1)	6 (5)	H(P2)	−0.09 (2)	0.39 (2)	0.17 (1)	6 (5)
H(4)	0.05 (2)	0.21 (1)	0.05 (1)	5 (4)	H(P3)	−0.31 (2)	0.29 (2)	0.30 (2)	8 (5)
H(5)	−0.22 (2)	0.05 (2)	0.11 (1)	6 (4)	H(P4)	−0.15 (2)	0.21 (2)	0.46 (1)	7 (5)
H(6)	−0.03 (2)	−0.03 (1)	0.36 (1)	5 (4)	H(P5)	0.09 (3)	0.26 (3)	0.51 (2)	9 (7)
H(P1)	0.14 (2)	0.39 (1)	0.34 (1)	5 (4)					

[a] The form of the anisotropic thermal parameter is $\exp[-2\pi^2(U_{11}h^2a^{*2} + U_{22}k^2b^{*2} + U_{33}l^2c^{*2} + 2U_{12}hka^*b^* + 2U_{13}hla^*c^* + 2U_{23}klb^*c^*)]$. For hydrogen atoms, standard isotropic B values are given.

Hg···X interactions,[15] as shown by Hg–X distances significantly less than the sum of van der Waals radii (4.10 Å for Hg and Cl). Thus, in $HgCl_2$ itself[16] each mercury atom is surrounded by three pairs of chlorine atoms at distances of 2.25, 3.34, and 3.63 Å, the last two being intermolecular.

In both VIB and VIIA, the mercury atom is regarded as sp hybridized and is linearly bonded to its coordinated ligands. As indicated in Table VII, the corresponding distances in the two structures are, in general, closely similar though there are a few differences; thus, the mercury atom is slightly closer to the carborane cage in VIB than in VIIA. The similarity of the molecules is particularly evident in a comparison of the dihedral angles between mean planes, as given in Table IX.

However, a notable exception is found in the positions of the B–H–B hydrogen bridges [H(56)]. In compound VIB, the dihedral angle subtended by the B(5)–H(56)–B(6) plane and the C_2B_3 ring is 46.2°, whereas in VIIA it is 66.5°; the difference is shown more dramatically by the deflection of H(56) from the Co–B(5)–B(6) plane, which in VIB is 9.5° outward (*away* from Hg) but in VIIA it is 10.9° inward (*toward* Hg) as shown in Figure 6. As a consequence, the H(56)–Hg distance is only 2.42 (9) Å in VIIA as compared to 2.79 (9) Å in VIB. While the determination of hydrogen atoms in the vicinity of mercury from X-ray data must be viewed with considerable caution, there are strong indications that the effect shown in Figure 6 is real. First, the ^{1}H NMR spectra of both VIB and VIIA exhibit ^{199}Hg satellites on the H(56) resonance, but the magnitude of the ^{199}Hg–^{1}H coupling constant (J) is larger in VIIA (113 Hz) than in VIB (67 Hz). Second, in VIIA, not only is the B–H–B bridge tilted toward Hg as suggested above, but in addition H(56) is skewed toward B(5), the boron adjacent to mercury; thus, B(5)–H(56) is 1.55 (1)

(15) (a) Seyferth, D. *J. Organomet. Chem.* **1973**, *62*, 33; **1974**, *75*, 13; **1975**, *98*, 133; **1977**, *143*, 153.
(16) (a) Braekken, H.; Scholten, W. *Z. Kristallogr., Kristallgeom., Kristallphys., Kristallchem.* **1934**, *89*, 448. (b) Grdenić, D. *Ark. Kemi* **1950**, *2*, 14.

Table VII. Interatomic Distances (Å) for μ-[(η^5-$C_5(CH_3)_5$)$Co(CH_3)_2C_2B_3H_4$]HgCl (VIB) and μ,μ'-[(η^5-C_5H_5)$Co(CH_3)_2C_2B_3H_4$]$_2$Hg (VIIA)

	VIB	VIIA
Hg–Cl	2.349 (3)	
Hg–Cl[a]	3.155 (3)	
Hg–Hg[a]	4.10	
Hg–B(4)	2.207 (13)	2.277 (8)
Hg–B(5)	2.289 (15)	2.355 (9)
Hg–H(56)	2.79 (9)	2.42 (9)
Co–C(P1)	2.059 (12)	2.047 (9)
Co–C(P2)	2.080 (11)	2.050 (9)
Co–C(P3)	2.068 (10)	2.024 (11)
Co–C(P4)	2.023 (11)	2.037 (10)
Co–C(P5)	2.039 (9)	2.052 (10)
⟨Co–C(P)⟩	2.05	2.05
Co–C(2)	2.045 (11)	2.047 (8)
Co–C(3)	2.043 (10)	2.059 (10)
Co–B(4)	2.093 (28)	2.037 (8)
Co–B(5)	2.036 (13)	2.045 (8)
Co–B(6)	2.025 (13)	2.075 (10)
C(2)–C(3)	1.347 (16)	1.428 (12)
C(3)–B(4)	1.632 (17)	1.586 (12)
B(4)–B(5)	1.717 (20)	1.723 (12)
B(5)–B(6)	1.786 (37)	1.848 (12)
B(6)–C(2)	1.486 (25)	1.521 (11)
C(2)–C(B2,M2)	1.652 (18)	1.535 (11)
C(3)–C(B3,M3)	1.494 (16)	1.499 (16)
B(5)–H(56)	1.531 (18)	1.549 (9)
B(6)–H(56)	1.362 (26)	1.629 (9)
C(P1)–C(P2)	1.332 (16)	1.349 (14)
C(P2)–C(P3)	1.421 (17)	1.373 (15)
C(P3)–C(P4)	1.455 (17)	1.298 (17)
C(P4)–C(P5)	1.415 (16)	1.394 (17)
C(P5)–C(P1)	1.346 (15)	1.424 (16)
⟨C(P)–C(P)⟩	1.39	1.37
C(P1)–C(M1)	1.569 (18)	
C(P2)–C(M2)	1.518 (16)	
C(P3)–C(M3)	1.506 (18)	
C(P4)–C(M4)	1.477 (17)	
C(P5)–C(M5)	1.598 (16)	
⟨C(P)–C(M)⟩	1.53	

[a] Intermolecular distance.

Å while B(6)–H(56) is 1.63 (1) Å. In VIB the opposite is true, as shown by the B(5)–H(56) and B(6)–H(56) distances of 1.53 (2) and 1.36 (1) Å, respectively. In both structures, the B–Hg–B bridge is significantly asymmetric, with Hg closer to B(4) than to B(5), but the Hg–B(5) distance is longer in VIIA than in VIB.

All of these observations are consistent with a weak, but real, bonding interaction between mercury and the bridging hydrogen atom in VIIA. We emphasize that it is *weak*, since the 2.42-Å Hg···H distance is 0.6 Å larger than the sum of covalent radii for Hg and H. It is nonetheless interesting to note that in the copper-bridged species[17] μ-[$(C_6H_5)_3P]_2Cu$-$B_5H_8Fe(CO)_3$, in which an established Cu···H interaction exists, the Cu–H distance (1.96 Å) is 0.5 Å greater than the sum of the covalent radii. In the copper complex, the bridging Cu attracts a *terminal* B–H hydrogen whereas in the present species VIIA, the bridging Hg interacts with a *bridging* hydrogen. It is not obvious why this effect should be felt more strongly in VIIA than in VIB, but we can eliminate direct H(56)···Cl (intermolecular) linkage in VIB inasmuch as that distance (3.54 Å) is far too great for even a weak bonding interaction.

The locations of the methyl groups in VIB and VIIA require comment. Hoffman, Mingos, and co-workers[18] have shown that when polyene or polyenyl ligands $(CR)_n$ n = 3–8, are face bonded to a metal atom, the R substituents will tend to bend either toward or away from the metal atom depending on ring size (n). The effect arises from the optimization of the overlap of polyene bonding MO's with the metal d orbitals, and it has been calculated that for $n > 5$ the substituents will tilt toward the metal while for $n < 5$ they will bend away. When n = 5, either is possible and structure determinations have produced examples[18] of both types of bending. In the present species VIB, the methyl groups on the $C_5(CH_3)_5$ ring show an average tilt of 3° away from the cobalt atom.

Somewhat surprisingly, in both VIB and VIIA the methyl groups on the C_2B_3 rings all tilt *toward* the cobalt atom, i.e., by 4.6 and 4.8° in VIB and by 5.8 and 8.4° in VIIA. This observation is curious since the $C_5R_5^-$ and $(CH_3)_2C_2B_3H_4^{3-}$ ligands are formally isoelectronic and, one would assume, roughly isolobal. Moreover, in VIB the $C_5(CH_3)_5$ and $(CH_3)_2C_2B_3H_3$ rings are nearly eclipsed, so that the bend of the carboranyl methyl groups occurs despite a repulsive steric interaction, albeit a weak one with an intermethyl C–C distance of ca. 3.9 Å.

Finally, we comment briefly on the observation of a single conformer in the bis(cobaltacarboranyl)mercury complex VIIA. Since the (η^5-C_5H_5)$Co(CH_3)_2C_2B_4H_5^-$ ligand occurs as a racemic mixture, complexation of two such groups to mercury via B–Hg–B bridging should generate two distinguishable stereoisomers, one of which would have idealized C_2 symmetry (the one observed as VIIA). In the other, the

Table VIII. Bond Angles (Deg) for VIB and VIIA

	VIB	VIIA
B(4)–Hg–B(5)	44.9 (5)	43.6 (3)
Cl–Hg–B(4)	156.0 (4)	
Cl–Hg–B(5)	157.3 (4)	
Cl–Hg–Cl[a]	84.9 (3)	
Cl[a]–Hg–B(4)	98.0 (3)	
Cl[a]–Hg–B(5)	103.5 (4)	
Hg–Cl–Hg[a]	95.1 (3)	
C(2)–Co–C(3)	38.5 (5)	40.7 (3)
C(3)–Co–B(4)	47.3 (5)	45.6 (3)
B(4)–Co–B(5)	50.0 (6)	49.9 (3)
B(5)–Co–B(6)	51.3 (9)	53.3 (4)
B(6)–Co–C(2)	41.5 (7)	43.3 (3)
C(2)–C(3)–B(4)	110.7 (10)	112.5 (7)
C(3)–B(4)–B(5)	101.6 (10)	106.3 (6)
B(4)–B(5)–B(6)	104.1 (12)	100.6 (6)
B(5)–B(6)–C(2)	99.2 (19)	102.7 (7)
B(6)–C(2)–C(3)	124.0 (18)	117.9 (7)
C(3)–C(2)–C(B2,M2)	112.5 (16)	120.4 (8)
B(6)–C(2)–C(B2,M2)	122.5 (19)	120.9 (8)
C(2)–C(3)–C(B3,M3)	127.3 (14)	121.2 (8)
B(4)–C(3)–C(B3,M3)	121.9 (14)	125.8 (8)
B(5)–H(56)–B(6)	76.0 (15)	71.1 (5)
Hg–B(4)–C(3)	111.3 (8)	115.9 (5)
Hg–B(4)–B(5)	70.1 (7)	70.6 (4)
Hg–B(5)–B(4)	65.1 (7)	65.8 (4)
Hg–B(5)–B(6)	115.7 (11)	115.3 (5)
C(P1)–C(P2)–C(P3)	109.7 (11)	108.4 (11)
C(P2)–C(P3)–C(P4)	105.9 (95)	109.9 (11)
C(P3)–C(P4)–C(P5)	104.0 (11)	109.3 (10)
C(P4)–C(P5)–C(P1)	110.8 (10)	105.4 (10)
C(P5)–C(P1)–C(P2)	109.5 (12)	106.8 (10)
⟨C(P)–C(P)–C(P)⟩	108	108
C(P5)–C(P1)–C(M1)	125.1 (14)	
C(P2)–C(P1)–C(M1)	125.2 (15)	
C(P1)–C(P2)–C(M2)	128.7 (17)	
C(P3)–C(P2)–C(M2)	121.5 (16)	
C(P2)–C(P3)–C(M3)	126.2 (17)	
C(P4)–C(P3)–C(M3)	127.7 (18)	
C(P3)–C(P4)–C(M4)	127.3 (16)	
C(P5)–C(P4)–C(M4)	128.3 (16)	
C(P4)–C(P5)–C(M5)	126.1 (15)	
C(P1)–C(P5)–C(M5)	123.1 (15)	
⟨C(P)–C(P)–C(M)⟩	126	

[a] Intermolecular Hg–Cl interaction.

(17) Mangion, M.; Ragaini, J. D.; Schmitkons, T. A.; Shore, S. G. *J. Am. Chem. Soc.* **1979**, *101*, 754.
(18) Elian, M.; Chen, M. M. L.; Mingos, D. P. M.; Hoffmann, R. *Inorg. Chem.* **1976**, *15*, 1148.

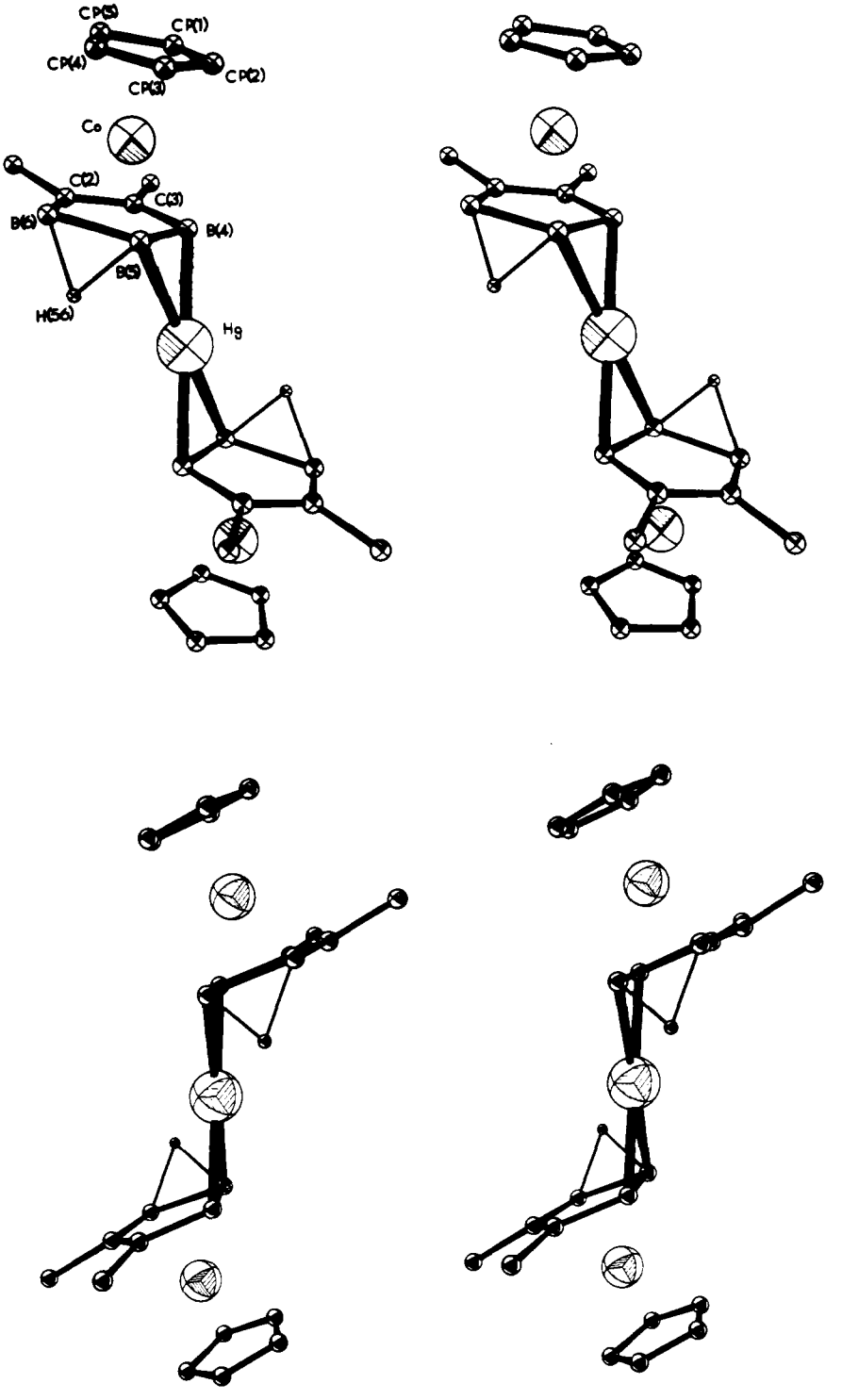

Figure 3. Stereoviews of the molecular structure of VIIA, with atoms shown as spheres of arbitrary radius.

bridging Hg and H atoms on one ligand are reversed relative to VIIA, producing idealized C_s (mirror) symmetry. In each of these isomers, which are analogous to those proposed for μ,μ'-$(C_2B_4H_7)_2SiH_2$,[4a] there is presumably free rotation about the mercury atom, thus giving rise to a number of different conformers in solution.

One must assume that both the C_2 and C_s stereoisomers are produced during synthesis, although they are probably indistinguishable via NMR spectroscopy, as in the case[2] with the bis(carboranyl)mercury complex (I) mentioned earlier. Hence, the fact that only the C_2 isomer of VIIA is observed in the crystal structure analysis must reflect differences in the molecular packing of the two forms. Conceivably the C_2 isomer crystallizes more readily or was fortuitously present in the crystal selected for data collection.

As compounds VIB and VIIA are the first metallacarboranes containing B–Hg–B bridge bonds to be crystallographically characterized, further exploration of these stereochemical effects must await additional structure determinations in this class of compounds.

Experimental Section

Materials. Pentamethylcyclopentadiene (Alfa) was used as received, and all other chemicals were reagent grade. Tetrahydrofuran (THF) was rigorously dried over $LiAlH_4$ prior to use. *n*-Butyllithium was obtained from Alfa as a hexane solution and determined to be 1.8 M by the method of Silveira.[19] NaH (Alfa, 50% in mineral oil) was

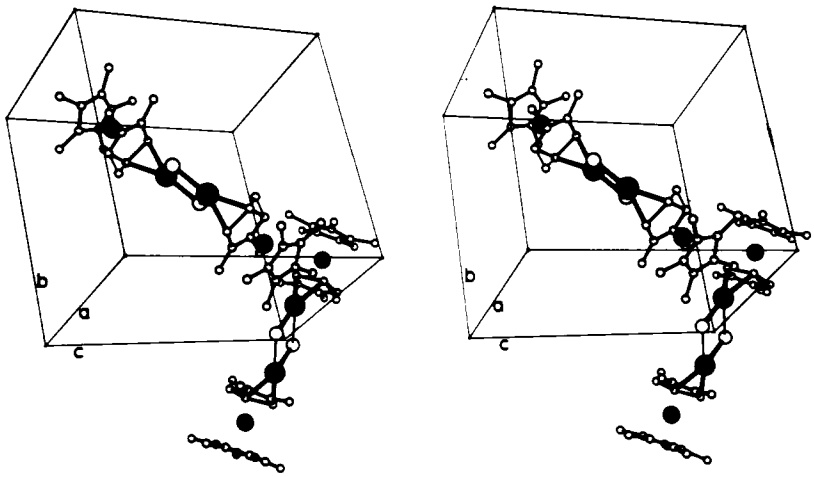

Figure 4. Unit cell packing in VIB.

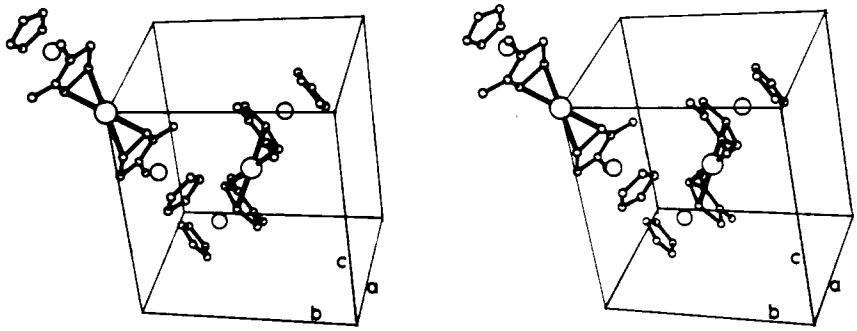

Figure 5. Unit cell packing in VIIA.

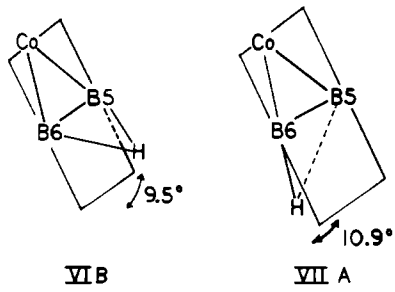

VI B VII A

Figure 6. Displacement of the bridging hydrogen atom H(56) out of the Co–B(5)–B(6) plane in VIB and VIIA.

washed with pentane prior to use. $(\eta^5\text{-}C_5H_5)Co(CH_3)_2C_2B_3H_5$ was prepared as described below, and $[\eta^5\text{-}C_5(CH_3)_5]Co(CH_3)_2C_2B_3H_5$ was similarly prepared as described elsewhere.[11] Thin-layer chromatography (TLC) was conducted on precoated plates of silica gel F-254 (Brinkmann Instruments, Inc.).

Instrumentation. ^{11}B (32 MHz) and ^1H (100 MHz) pulse Fourier transform NMR spectra were recorded on a JEOL PS-100P spectrometer interfaced to a JEOL-Texas Instruments EC-100 computer system. Broad-band heternuclear decoupling was employed. Unit-resolution mass spectra (EI) were obtained on a Hitachi Perkin-Elmer RMU-6E mass spectrometer. Infrared spectra were recorded on a Beckman IR-8 instrument.

Synthesis of $(\eta^5\text{-}C_5H_5)Co(CH_3)_2C_2B_3H_5$ (III). $(\eta^5\text{-}C_5H_5)Co(CH_3)_2C_2B_3H_5$ was prepared via degradation of $(\eta^5\text{-}C_5H_5)Co(CH_3)_2C_2B_4H_4$ in basic THF or CH_3CN.[10] In a typical reaction, about 250 mg of $(\eta^5\text{-}C_5H_5)Co(CH_3)_2C_2B_4H_4$ was dissolved in 20 mL of CH_3CN to which 15 mL of 2 M NaOH was added with stirring. The progress of the reaction was monitored by spot TLC in 1:1 CH_2Cl_2/hexane solutions [1,2,3-$(\eta^5\text{-}C_5H_5)Co(CH_3)_2C_2B_4H_4$, R_f = 0.6; III, R_f = 0.9], and after 1 h the reaction was stopped by removal of most of the CH_3CN by rotary evaporation. The cobaltacarboranes were extracted from the remaining slurry with CH_2Cl_2 and purified by TLC to give about 200 mg of III (83% yield) and a small amount of the starting material. Use of THF instead of CH_3CN generally gave a lower yield of III (50%) and trace yields of the other characterized cobaltacarboranes,[10,20] 1,7,2,3-$(\eta^5\text{-}C_5H_5)_2Co_2(CH_3)_2C_2B_3H_3$ and $(\eta^5\text{-}C_5H_5)_2Co_2(CH_3)_4C_4B_6H_6$ (isomer V).

Synthesis of (Pentamethylcyclopentadienyl)cobaltacarboranyl–Mercury Compounds (VIB, VIIB). A tip-in side-arm flask was charged with 60 mg (0.21 mmol)[11] of $[\eta^5\text{-}C_5(CH_3)_5]Co(CH_3)_2C_2B_3H_5$, (IV) and 50 mg of NaH (0.25 mmol). The flask was evacuated, and about 20 mL of dry THF was distilled in vacuo into the flask at −196 °C. The flask was warmed to 23 °C with no reaction (yellow solution) and then warmed to 60 °C for 15 min with no reaction. The solution was allowed to stir at 23 °C for 12 h (giving a yellow-orange color) whereupon it was filtered in vacuo into a flask containing 67 mg of $HgCl_2$ (0.25 mmol). With no immediate reaction being observed, the solution was stirred for 2 days at 23 °C, producing a dark, flocculent yellow suspension and a gray precipitate. The THF was removed in vacuo, and the system was exposed to the air. Extracts using CH_2Cl_2 and hexane were purified via TLC to give 22 mg of yellow-orange μ,μ'-$[(\eta^5\text{-}C_5(CH_3)_5)Co(CH_3)_2C_2B_3H_4]_2Hg$ (VIIB; 0.028 mmol, 27% yield; R_f = 0.2 in hexane; m/e 772; mp = 255 °C dec), 34 mg of yellow-orange μ-$(\eta^5\text{-}C_5(CH_3)_5)Co(CH_3)_2C_2B_3H_4HgCl$ (VIB; 0.065 mmol, 31% yield; R_f = 0.5 in 1:1 CH_2Cl_2/hexane; m/e 524; mp = 173 °C dec), 3 mg of the starting material, and a trace of VB, formulated as the sodium salt of the adduct $[(\eta^5\text{-}C_5(CH_3)_5)Co(CH_3)_2C_2B_3H_4{\cdot}HgCl_2]^-$ (R_f = 0.05 in 1:1 CH_2Cl_2/hexane). All of these compounds are moderately air-stable; the slow decomposition of VB to VIB has been noted.

A similar reaction, in which the NaH deprotonation step involved stirring for 2 h (possibly incomplete) and the reaction with $HgCl_2$ was stirred for only 10 min, gave a 4.3% yield of VIB, a 19% yield of VB, and a 49% recovery of the starting compound. Other compounds (in trace yield) of similar color and R_f as that of VB gave

(19) Silveira, A. D., Jr.; Bretherick, H. D., Jr.; Negishi, E. *J. Chem. Educ.* **1979**, *56*, 569.

(20) Wong, K.-S.; Bowser, J. R.; Pipal, J. R.; Grimes, R. N. *J. Am. Chem. Soc.* **1978**, *100*, 5045.

Table IX. Least-Squares Planes for VIB and VIIA with Deviations of Selected Atoms (Å)

μ-[(η^5-$C_5(CH_3)_5$)Co$(CH_3)_2C_2B_3H_4$]HgCl (VIB)

Plane 1 (VIB): C(P1), C(P2), C(P3), C(P4), C(P5)

$0.4809x + 0.8193y - 0.3123z - 6.9441 = 0$

C(P1)	−0.0148	C(P5)	0.0208	C(M3)	0.1421
C(P2)	0.0023	Co	−1.6760	C(M4)	0.0603
C(P3)	0.0097	C(M1)	0.0239	C(M5)	0.0884
C(P4)	−0.0180	C(M2)	0.0859		

Plane 2 (VIB): C(2), C(3), B(4), B(5), B(6)

$0.3703x + 0.8678y - 0.3314z - 3.8037 = 0$

C(2)	−0.0306	B(5)	−0.0297	Co	1.5358
C(3)	0.0054	B(6)	0.0360	C(B2)	0.1329
B(4)	0.0189	Hg	−1.9580	C(B3)	0.1241

Plane 3 (VIB): Hg, B(4), B(5)

$-0.7530x - 0.2881y - 0.5915z + 1.3967 = 0$

Cl	−0.2730

Plane 4 (VIB): Co, B(4), B(5)

$-0.7663x - 0.4695y - 0.4386z + 2.1944 = 0$

Hg	0.4896

Plane 5 (VIB): B(5), B(6), H(56)

$0.8420x + 0.2565y - 0.4745z - 3.5713 = 0$

Plane 6 (VIB): Co, B(5), B(6)

$0.8750x + 0.0947y + 0.4747z - 3.2279 = 0$

H(56)	0.1864

Plane 7 (VIB): Hg, Cl, Cl*

$0.5341x - 0.6067y - 0.5888z = 0$

μ,μ'-[(η^5-C_5H_5)Co$(CH_3)_2C_2B_3H_4$]$_2$Hg (VIIA)

Plane 1 (VIIA): C(P1), C(P2), C(P3), C(P4), C(P5)

$0.4260x - 0.7830y - 0.4532z + 5.0877 = 0$

C(P1)	0.0078	C(P3)	0.0082	C(P5)	−0.0029
C(P2)	−0.0099	C(P4)	−0.0032	Co	1.6784

Plane 2 (VIIA): C(2), C(3), B(4), B(5), B(6)

$0.3585x - 0.8022y - 0.4774z - 1.9800 = 0$

C(2)	0.0011	B(6)	−0.0043	H(56)	1.1856
C(3)	0.0034	Hg	1.9800	C(M2)	−0.2250
B(4)	−0.0058	Co	−1.5174	C(M3)	−0.1504
B(5)	0.0056				

Plane 3 (VIIA): Hg, B(4), B(5)

$0.5589x + 0.5828y - 0.5899z = 0$

Plane 4 (VIIA): Co, B(4), B(5)

$-0.5802x + 0.7009y - 0.4148z - 0.4533 = 0$

Hg	−0.4533

Plane 5 (VIIA): B(5), B(6), H(56)

$0.9556x + 0.0956y - 0.2788z + 1.5284 = 0$

Plane 6 (VIIA): Co, B(5), B(6)

$0.9339x - 0.0801y - 0.3484z + 1.7815 = 0$

H(56)	0.2446

Dihedral Angles (Deg)

compd VIB		compd VIIA	
planes	angle	planes	angle
1,2	7.01	1,2	4.25
2,3	70.56	2,3	67.27
3,4	13.65	3,4	12.19
5,6	9.47	5,6	10.92
2,5	46.24	2,5	66.49
3,7	83.06		

mass spectra indicating the addition of extra chlorine atoms.

Synthesis of Cyclopentadienylcobaltacarboranyl–Mercury Compounds (VIA, VIIA). The syntheses are similar to those described above for VIB and VIIB. In dry THF, 50 mg of (η^5-C_5H_5)Co$(CH_3)_2C_2B_3H_5$ (III; 0.23 mmol) was deprotonated in vacuo with 55 mg of NaH (2.3 mmol) over a period of 30 min with H_2 evolution and a color change from yellow to orange. After freezing the solution, the H_2 (not measured) was removed by evacuation. The salt was then filtered at 23 °C in vacuo into a flask containing 63 mg of $HgCl_2$ (0.23 mmol), effecting an immediate color change back to yellow. The solution was stirred for 10 min at 23 °C and the THF removed in vacuo. The flask was exposed to the air, and CH_2Cl_2 and hexane extracts were purified via TLC to give 48 mg of yellow-orange μ,μ'-[(η^5-C_5H_5)Co$(CH_3)_2C_2B_3H_4$]$_2$Hg (VIIA; 0.076 mmol, 66% yield; R_f = 0.2 in hexane, 0.85 in 1:1 CH_2Cl_2/hexane; m/e 632, mp = 190 °C dec), a trace of yellow-orange μ-[(η^5-C_5H_5)Co$(CH_3)_2C_2B_3H_4$]HgCl (VIA; R_f = 0.7 in 33% acetone in hexane; m/e 452), a trace of starting material, and salts analogous to those described above (R_f = 0.2–0.3 in 1:1 CH_2Cl_2/hexane).

A similar reaction conducted over a period of 4 days gave no compounds in isolable yields.

X-ray Crystal Structure Determinations on VIB and VIIA. The crystals used were grown by slow evaporation of solvent: compound VIB from 10% CH_2Cl_2 in hexane at 10 °C and compound VIIA from CH_2Cl_2 at 10 °C. The crystals were mounted on glass fibers in arbitrary orientations and examined by preliminary precession photographs which indicated acceptable crystal quality. Crystal data for $HgCoClC_{14}B_3H_{25}$ (VIB): mol wt 520.76; space group $P2_1/n$; Z = 2; a = 9.634 (2), b = 14.046 (10), c = 13.862 (7) Å; β = 96.71 (3)°; V = 1863 Å^3; μ(Mo Kα) = 94.6 cm^{-1}; ρ(calcd) = 1.86 g cm^{-1}. Crystal dimensions (mm from centroid): (010) 0.06, (0$\bar{1}$0) 0.06, (101) 0.125, ($\bar{1}$0$\bar{1}$) 0.125, (10$\bar{1}$) 0.14, ($\bar{1}$01) 0.14. Crystal data for $HgCo_2C_{18}B_6H_{30}$ (VIIA): mol wt 629.75; space group $P2_1/n$; Z = 2; a = 8.456 (8), b = 11.334 (7), c = 11.77 (1) Å; β = 100.12 (9)°; V = 1110 Å^3; μ(Mo Kα) = 85.8 cm^{-1}; ρ(calcd) = 1.88 g cm^{-1}. Crystal dimensions (mm from centroid): (100) 0.06, ($\bar{1}$00) 0.06, (011) 0.145, (0$\bar{1}\bar{1}$) 0.145, (01$\bar{1}$) 0.145, (0$\bar{1}$1) 0.145.

For each crystal the Enraf-Nonius program SEARCH was used to obtain 25 accurately centered reflections which were then used in the program INDEX to obtain an orientation matrix for data collection and to provide approximate cell dimensions. Refined cell dimensions and their estimated standard deviations were obtained from 28 accurately centered reflections. The mosaicity of the crystals was examined by the ω-scan technique and judged to be satisfactory. The space groups were chosen on the basis of systematic absences and chemical and spectroscopic information. In each case, successful solution and refinement of the structure confirmed the choice of space group.

Collection and Reduction of the Data. Diffraction data were collected at 295 K on an Enraf-Nonius four-circle CAD-4 diffractometer controlled by a PDP8/M computer using Mo Kα radiation from a highly oriented graphite-crystal monochrometer. The θ–2θ scan technique was used to record the intensities of all reflections for which $1.0 < 2\theta < 48°$ for VIB and $1.0 < 2\theta < 50°$ for VIIA. Scan widths were calculated from the formula SW = $(A + B \tan \theta)°$, where A is estimated from the mosaicity of the crystal and B compensates for the increase in the width of the peak due to Kα_1–Kα_2 splitting. The values of A and B are 0.60 and 0.35 for VIB and 0.60 and 0.30 for VIIA, respectively. The calculated scan angle was extended at each side by 25% for background determination (BG1 and BG2). The net count (NC) was then calculated as NC = TOT − 2(BG1 + BG2), where TOT is the estimated peak intensity.

The intensities of four standard reflections, at 100-reflection intervals, showed no greater fluctuations during the data collection than those expected from Poisson statistics. The raw intensity data were corrected for Lorentz–polarization effects and then for absorption (minimum transmission factor 0.21, maximum 0.55 for VIB; minimum 0.28, maximum 0.46 for VIIA), resulting in 2274 reflections for VIB and 1851 reflections for VIIA, of which 1607 for VIB and 1441 for VIIA had $F_o^2 > 3\sigma(F_o^2)$, where $\sigma(F_o)$ was estimated from counting statistics (p = 0.03).[21] Only the 3σ data were used in the final refinement of the structural parameters.

Solution and Refinement of the Structures. Full-matrix least-squares refinement was based on F, and the function minimized was $w(|F_o| - |F_c|)^2$. The weights w were taken as $[2F_o/\sigma(F_o^2)]^2$, where $|F_o|$ and $|F_c|$ are the observed and calculated structure factor amplitudes. The atomic scattering factors for nonhydrogen atoms were taken from Cromer and Waber[22] and those for hydrogen from Stewart et al.[23]

(21) Corfield, P. W. R.; Doedens, R. J.; Ibers, J. A. *Inorg. Chem.* **1967**, *6*, 197.

(22) Cromer, D. T.; Waber, J. T. "International Tables for X-ray Crystallography"; Kynoch Press: Birmingham, England, 1974; Vol. IV.

The effects of anomalous dispersion for all nonhydrogen atoms were included in F by using the values of Cromer and Ibers[24] for $\Delta f'$ and $\Delta f''$.

The positions of the mercury and cobalt atoms in VIB were determined from three-dimensional Patterson functions calculated from all intensity data. The intensity data were phased sufficiently well by these positional coordinates to permit location of the remaining nonhydrogen atoms from Fourier difference functions. A small amount of positional disorder was observed in the $(CH_3)_5C_5$ ring, but the disordered positions could not be adequately established and contributed little to the overall scattering. This disorder is also unimportant in terms of the interesting structural features of the molecule and was therefore not pursued further. The molecule was found to be dimerized about a crystallographic inversion center via a pair of Hg-Cl interactions. Anisotropic temperature factors were introduced for all nonhydrogen atoms. The position of the bridging hydrogen, H(56), was calculated and included in the refinement, except during the final three cycles. A final Fourier difference map was featureless. The esd of an observation of unit weight was 2.49.

For compound VIIA the positions of the cobalt and mercury atoms were determined from a three-dimensional Patterson function. The Hg atom was found to be at a center of inversion, thus requiring solution for only half of the molecule. The intensity data were phased sufficiently well by the coordinates of the Hg and Co atoms to permit location of the remaining nonhydrogen atoms from Fourier difference functions. After introducing anisotropic thermal parameters for all nonhydrogen atoms, some hydrogen atoms were found on Fourier difference maps, and those remaining were calculated and inserted. All hydrogen atoms were included in the refinement for three cycles and thereafter held fixed. A final Fourier difference map was featureless. The esd of an observation of unit weight was 4.62.

The models converged to $R = 0.044$ and $R_w = 0.055$ for VIB and $R = 0.081$ and $R_w = 0.094$ for VIIA, where $R = \sum||F_o| - |F_c||/\sum|F_o|$ and $R_w = [\sum w(|F_o| - |F_c|)^2/\sum w|F_o|^2]^{1/2}$. Tables of observed and calculated structure factors are available (see paragraph at end of paper regarding supplementary material). The computing system and programs are described elsewhere.[25]

Acknowledgment. This work was supported by the Office of Naval Research and the National Science Foundation, Grant No. 79-09948. We are grateful to Professor Ekk Sinn for assistance in the X-ray crystallographic structure determinations.

Registry No. III, 65969-67-7; IV, 76095-34-6; VA, 76081-87-3; VB, 76081-88-4; VIA, 76081-89-5; VIB, 76081-90-8; VIIA, 76190-15-3; VIIB, 76190-16-4; $(\eta^5\text{-}C_5H_5)Co(CH_3)_2C_2B_4H_4$, 50932-66-6; $HgCl_2$, 7487-94-7.

Supplementary Material Available: Listings of observed and calculated structure factor amplitudes (14 pages). Ordering information is given on any current masthead page.

(23) Stewart, R. F.; Davidson, E. R.; Simpson, W. T. *J. Chem. Phys.* **1965**, *42*, 3175.
(24) Cromer, D. T.; Ibers, J. A. Reference 22.
(25) Freyberg, D. P.; Mockler, G. M.; Sinn, E. *J. Chem. Soc., Dalton Trans.* **1976**, 447.

Contribution from the Department of Chemistry and Molecular Structure Center, Indiana University, Bloomington, Indiana 47405

Reactions of Metal-Metal Multiple Bonds. 7.[1] Addition of the Halogens Cl_2, Br_2, and I_2 and Diisopropyl Peroxide to Hexaisopropoxydimolybdenum (M≡M). Dinuclear Oxidative-Addition Reactions Accompanied by Metal-Metal Bond-Order Changes from 3 to 2 to 1

MALCOLM H. CHISHOLM,* CHARLES C. KIRKPATRICK, and JOHN C. HUFFMAN

Received September 19, 1980

$Mo_2(O\text{-}i\text{-}Pr)_6$ (M≡M) and *i*-PrOO-*i*-Pr react in hydrocarbon solvents, at room temperatures, and in the dark to give the previously characterized compound $Mo_2(O\text{-}i\text{-}Pr)_8$ (M=M). $Mo_2(O\text{-}t\text{-}Bu)_6$ (M≡M) fails to react with either *i*-PrOO-*i*-Pr or *t*-BuOO-*t*-Bu, and $Mo_2(O\text{-}i\text{-}Pr)_6$ and *t*-BuOO-*t*-Bu do not react under similar conditions. A reaction pathway involving an initial association reaction is proposed: $Mo_2(OR)_6 + ROOR \rightleftharpoons Mo_2(OR)_6(ROOR) \rightarrow Mo_2(OR)_8$. $Mo_2(O\text{-}i\text{-}Pr)_6$ reacts with each of the halogens Cl_2, Br_2, and I_2 to give $Mo_2(O\text{-}i\text{-}Pr)_6X_4$ (M—M) compounds (X = Cl, Br, and I). These reactions proceed via intermediates, probably $Mo_2(O\text{-}i\text{-}Pr)_6X_2$ compounds, which are labile toward disproportionation to give $Mo_2(O\text{-}i\text{-}Pr)_6$ and $Mo_2(O\text{-}i\text{-}Pr)_6X_4$ compounds. The compounds $Mo_2(O\text{-}i\text{-}Pr)_6X_4$ are thermally unstable and moisture sensitive. In vacuo or under a nitrogen atmosphere they decompose slowly at room temperature by the elimination of isopropyl halides. X-ray studies on the chloro and bromo compounds show that both compounds contain central $Mo_2O_6X_4$ units that have virtual D_{2h} symmetry. Each molybdenum atom is in a distorted octahedral environment formed by a pair of cis terminal halide ligands, a pair of trans terminal O-*i*-Pr ligands, and a pair of cis-bridging O-*i*-Pr ligands. There are planar $Mo_2(\mu\text{-}O)_2X_4$ units and the M-M distance in both is 2.73 Å, which, together with other characterization data, are indicative of Mo-to-Mo single bonds. These findings are compared with earlier work. Crystal data are as follows: for $Mo_2(O\text{-}i\text{-}Pr)_6Cl_4$ $a = 20.722$ (6) Å, $b = 9.617$ (2) Å, $c = 14.747$ (4) Å, $\beta = 96.02$ (1)°, $V = 2922.6$ (1) Å^3, $Z = 4$, $d_{calcd} = 1.578$ g cm^{-3} with space group $P2_1/a$; for $Mo_2(O\text{-}i\text{-}Pr)_6Br_4 \cdot {}^1/_2C_7H_8$ $a = 15.204$ (5) Å, $b = 12.849$ (5) Å, $c = 10.535$ (3) Å, $\beta = 120.76$ (1)°, $V = 1768.6$ (1) Å^3, $Z = 4$, $d_{calcd} = 1.638$ g cm^{-3} with space group $P2_1/a$.

Introduction

In mononuclear transition-metal chemistry, the term oxidative addition[2] is often used to describe reactions in which both the oxidation number and coordination number of the metal are increased by 2. The microscopic reverse reaction is called reductive elimination, and the two complementary reactions are incorporated into numerous catalytic cycles, involving especially the group 8 transition elements.[2] We have speculated[3] that dinuclear compounds of the transition elements containing metal-to-metal triple bonds[4] might also enter into these types of reactions and that M-M bond-order changes

(1) Chisholm, M. H.; Cotton, F. A.; Extine, M. W.; Kelly, R. L. *J. Am. Chem. Soc.* **1979**, *101*, 7645.
(2) Tolman, C. A. *Chem. Soc. Rev.* **1972**, *1*, 337.
(3) Chisholm, M. H. *Transition Met. Chem. (Weinheim, Ger.)* **1978**, *3*, 321; *Adv. Chem. Ser.* **1979**, *No. 173*, 396.
(4) For recent reviews see: Cotton, F. A. *Chem. Soc. Rev.* **1975**, *4*, 27. Cotton, F. A. *Acc. Chem. Res.* **1978**, *11*, 226. Chisholm, M. H.; Cotton, F. A. *Ibid.*, **1978**, *11*, 356.

0020-1669/81/1320-0871$01.00/0